

N 70 18797
Nasa. TMX-53972

**NASA TECHNICAL
MEMORANDUM**

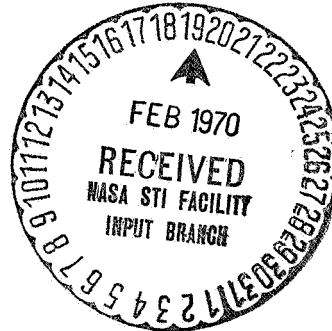
NASA TM X-53972

**CASE FILE
COPY**

**TRACTION DRIVE SYSTEM DESIGN CONSIDERATIONS
FOR A LUNAR ROVING VEHICLE**

By Clyde S. Jones, Jr., Billy J. Doran, and Frank J. Nola
Astrionics Laboratory

November 25, 1969



NASA

*George C. Marshall Space Flight Center
Marshall Space Flight Center, Alabama*

1. REPORT NO. TM X-53972	2. GOVERNMENT ACCESSION NO.	3. RECIPIENT'S CATALOG NO.	
4. TITLE AND SUBTITLE Traction Drive System Design Considerations for a Lunar Roving Vehicle		5. REPORT DATE November 25, 1969	
		6. PERFORMING ORGANIZATION CODE	
7. AUTHOR(S) Clyde S. Jones, Jr., Billy J. Doran, and Frank J. Nola		8. PERFORMING ORGANIZATION REPORT #	
9. PERFORMING ORGANIZATION NAME AND ADDRESS George C. Marshall Space Flight Center Marshall Space Flight Center, Alabama 35812		10. WORK UNIT NO.	
		11. CONTRACT OR GRANT NO.	
12. SPONSORING AGENCY NAME AND ADDRESS		13. TYPE OF REPORT & PERIOD COVERED Technical Memorandum	
		14. SPONSORING AGENCY CODE	
15. SUPPLEMENTARY NOTES Prepared by Advanced Research and Technology Branch, Guidance and Control Division, Astrionics Laboratory			
16. ABSTRACT <p>For an optimum design, the weight, energy consumption, and operational flexibility of the traction drive system for a lunar roving vehicle must be considered along with the power supply, motor, and power train.</p> <p>Other problems considered in this paper include: environment and motor dissipation, motor type (i.e., ac or dc) and commutation if dc, motor controller (i.e., switching of large currents), delivery of torque at varying speeds, power train, use of regenerative braking and conservation of energy, and power supply voltage variation. These problems are studied in view of certain general system specifications, which fall into weight, performance, and environment categories. Tradeoff studies are considered for optimization in each of these areas.</p> <p>Special consideration is given to the controller and system design as it pertains to regenerative braking and the conservation of energy. Some aspects of changing the modes of motor operation to satisfy extreme performance requirements of speed and torque are discussed.</p>			
17. KEY WORDS Brushless Motor Hall Effect Device Pulse Width Modulation Energy Requirements		18. DISTRIBUTION STATEMENT Announce in STAR	
19. SECURITY CLASSIF. (of this report) Unclassified	20. SECURITY CLASSIF. (of this page) Unclassified	21. NO. OF PAGES 35	22. PRICE \$ 3.00

TABLE OF CONTENTS

	Page
SUMMARY	1
INTRODUCTION	1
SYSTEM TRADEOFF CONSIDERATIONS	2
Drive Motor Selection	3
General Design Considerations	4
Battery Voltage Selection	6
Motor-Power Train Tradeoff	7
MOTOR-BATTERY TRADEOFF	8
Environmental Considerations	12
ADDITIONAL TECHNIQUES AND TRADEOFFS FOR REDUCING MOTOR WEIGHT AND CONTROLLER CURRENT.	13
CONSIDERATIONS FOR THE MOTOR CONTROLLER.	14
APPENDIX A: THE BRUSHLESS DC MOTOR	20
REFERENCES.	25

LIST OF ILLUSTRATIONS

Figure	Title	Page
1.	Traction drive system	2
2.	Motor controller equivalent circuit	4
3.	Motor weight versus gear ratio for MLRV	9
4.	Torque-speed curves for dc motor	10
5.	Series/parallel winding configuration	15
6.	Motor controller	17
A-1.	Hall effect device.	21
A-2.	Basic operation of motor.	22

DEFINITION OF SYMBOLS

Symbol	Definition
ω_w	Wheel speed
ω_{wm}	Maximum wheel speed
ω_m	Motor speed
ω_{mm}	Maximum motor speed
V_{bb}	Battery voltage
V_c	Voltage drop in the controller
I_m	Motor current
I_{mm}	Maximum motor current
R_m	Motor resistance
L_m	Motor inductance
V_b	Motor back emf or generated voltage
V_{bm}	Maximum motor back emf or generated voltage
K_b	Motor generator constant
K_t	Motor torque constant
T_m	Motor torque

DEFINITION OF SYMBOLS (Continued)

Symbol	Definition
T_{mm}	Maximum motor torque
N	Gear ratio
T_w	Wheel torque
T_{wm}	Maximum wheel torque
P_{mm}	Maximum power dissipation within the motor
W_m	Weight of motor
K_m	A constant associated with motor weight
W_b	Weight of battery
R_2	Resistance of motor winding at temperature T
R_1	Resistance of motor winding at temperature T_1
α_1	Temperature coefficient of resistance at T_1
$Q_1, Q_2,$ $Q_3 \dots Q_n$	Transistor designations
$D_1, D_2,$ $\dots D_n$	Diode designations
V_h	Voltage output from Hall effect device
B	Magnetic flux density
I_{ex}	Hall device excitation current

DEFINITION OF SYMBOLS (Concluded)

Symbol	Definition
α	Angular position of rotor
K_h	Hall device constant
K_a	Amplifier gain
K_w	Tachometer scale factor

TRACTION DRIVE SYSTEM DESIGN CONSIDERATIONS FOR A LUNAR ROVING VEHICLE

SUMMARY

With the constraint on weight, battery voltage, controller current, gear ratio, heat dissipation, and environment, the tradeoffs favor using an overrated brushless dc motor. Also the overrated motor has the advantage of being capable of satisfying more stringent torque-speed requirements. This would not be true of the minimum size permanent magnet motor or a series motor, which has been suggested by some. A winding shift is also a practical way of reducing controller current. The high-efficiency static controller using pulse width modulation minimizes the problem of heat dissipation, permits braking, and allows continuous operation with full torque if desired.

It is expected that these results, although they do not constitute a final design, will significantly influence the final system design that will be implemented on the manned lunar roving vehicle.

INTRODUCTION

A lunar roving vehicle (LRV) traction drive system depends upon a number of subsystems for its performance; therefore, each must be considered in the system design. An optimum design with respect to weight, energy requirements, and operational flexibility requires tradeoffs between the power supply, motor, motor controller, power train, and wheel. Certain constraints on the system, such as LRV weight and overall dimensions, are dictated by the delivery vehicle. Thus, the LRV weight and maximum wheel dimensions are specified and the traction drive is designed with these as inflexible constraints. Other constraints arise because of performance requirements. Two of these, the maximum vehicle velocity and stall torque capability, have a significant effect on the drive system design, especially in the motor-power train tradeoff studies. Hardware constraints are also imposed on the subsystem design and will be considered here.

Two distinct types of LRV's are now under consideration by NASA. One of these, the dual mode LRV (DMLRV), will have the capability of either manned or unmanned operation and is a very sophisticated vehicle for future lunar surface missions. The DMLRV is in the study phase and is not planned to reach the hardware phase until the mid 1970's. The other is the manned only LRV (MLRV), which is now entering the hardware phase. The MLRV will have a short operational life (approximately 78 hr) and will be small and lightweight. This relatively unsophisticated vehicle is scheduled for operation on the moon in 1971. Only the requirements for the MLRV are considered in sizing the motor and controller. However, since both vehicles have similar environmental requirements, the type of motor chosen will perform well on either vehicle.

SYSTEM TRADEOFF CONSIDERATIONS¹

Figure 1 is a block diagram of the traction drive system. Those subsystems that figure prominently in the design are shown in individual blocks.

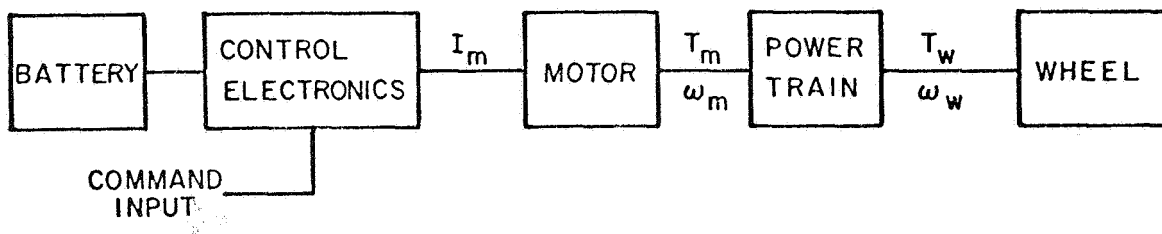


Figure 1. Traction drive system.

To arrive at a system design, assumptions are made based on the best information available. Vehicle parameters assumed are:

1. Number of wheels — 4.
2. Maximum wheel velocity — 11.0 rad/sec = 104 rpm.
3. Maximum vehicle earth weight — 181 + 408 (payload) = 589 kg (1300 lb).
4. Maximum torque required per wheel — 88 newton meters (65 lb-ft).

1. The design will be considered for only one wheel.

The subsystems shown in Figure 1 are interdependent. Thus, to achieve an optimal design with respect to weight and performance, tradeoff studies are required.

Drive Motor Selection

The choice of motor type is to some degree subjective since so many variations of both ac and dc motors are known; however, for this particular application, a reasonably justifiable selection rationale may be used. In-house studies and tradeoffs have led MSFC to the conclusion that the permanent magnet (PM) dc motor is the most efficient and reliable for the application [1].

Some of the reasons for this selection are given. First, minimizing system weight is the prime consideration in this design and the PM dc motor has a higher torque to weight ratio than comparable performance ac motors.² Secondly, speed and torque control techniques are less complicated and more reliable. Third, the total energy requirements are less since the primary power source is dc and no inverter with its attendant losses is necessary.³ The ac motor has the advantage of no mechanical contact, such as brushes; however, investigation into the problems of operating brushes in the space environment indicates that for short periods of time and relatively low brush-commutator velocity, brush technology is adequate. Performance at high brush-commutator velocity in the space environment has not been determined.

Present research work, both in-house and by contractor [3,4], has developed a very efficient compact brushless motor, which is discussed in more detail in the Appendix. Although the controller for the brushless motor is more complicated than for the brush motor, a by-product of the control technique

-
2. A possible candidate is the homopolar induction motor developed by the U.S. Army Tank Command described in Reference 2. MSFC has built a prototype motor using this principle, and although it offers some distinct advantages for land vehicles, it is believed that the development time required prohibits the use of this motor for the MLRV.
 3. This advantage is somewhat offset when considering the brushless PM dc motor because of its similarity to the ac motor in design of control electronics.

gives odometer and velocity information with only a slight increase in parts count. Present knowledge of lunar environmental conditions has caused MSFC to consider the use of the brushless motor since there are no technology problems to be solved. A significant advantage of the brushless motor for this application, aside from the elimination of brushes, is the superior thermal characteristics because the windings where heat is generated are located on the stator and can directly use the vehicle for a heat sink. This is made more significant since the operating environment is a vacuum in which the generation and dissipation of heat (controlling factor in a motor design) is acute.

General Design Considerations

Since the PM dc motor has been selected, some general system design criteria can be established. Assume for the initial design that a direct drive will be used (i.e., $\omega_{\text{wheel}} = \omega_{\text{motor}}$). A functional equivalent circuit for the motor-controller is illustrated in Figure 2.

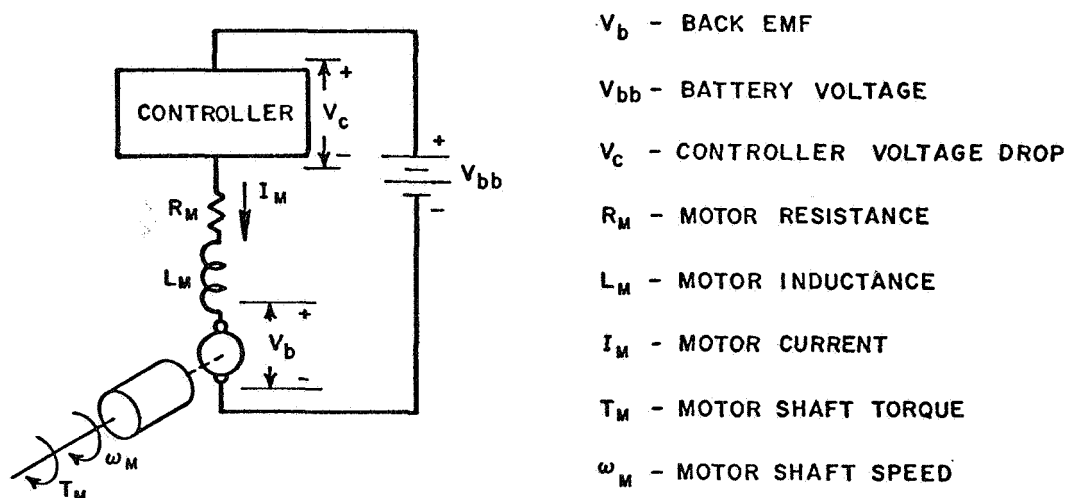


Figure 2. Motor controller equivalent circuit.

The linearized voltage-current relationships for this circuit is described by

$$V_{bb} = V_c + I_m R_m + L_m \frac{dI_m}{dt} + V_b \quad (1)$$

If the inductive voltage drop is neglected, the voltage available for back electromotive force (emf) can be expressed as:

$$V_b = V_{bb} - V_c - I_m R_m \quad (2)$$

V_c is a constant (2 to 3 V) and is independent of load current for the type of controller being considered (a pulse width modulation scheme will be used).

When the MLRV is running at maximum speed, V_{bb} must be sufficiently greater than V_b (max) to allow current to flow to overcome losses. With this in mind, an equation for current can be derived. Assuming that the power train contains no gear shift, the back emf constant is given by the expression

$$K_b = \frac{V_{bm}}{\omega_{mm}} \quad (3)$$

Since $K_b = K_t$ (the torque constant), in a consistent set of units, then

$$K_t = \frac{T_{mm}}{I_{mm}} = \frac{V_{bm}}{\omega_{mm}} \text{ and } I_{mm} = \frac{T_{mm} \omega_{mm}}{V_{bm}} = \frac{\left(\frac{T_{wm}}{n}\right) (n\omega_{wm})}{V_{bm}} \quad (4)$$

In these equations

$T_{wm} \triangleq$ maximum wheel stall torque in newton meters.

$T_{mm} \triangleq$ maximum motor stall torque in newton meters.

$\omega_{mm} \triangleq$ maximum no load motor angular velocity (radians/second)

$I_{mm} \triangleq$ maximum motor current in amperes.

$\omega_{wm} \triangleq$ maximum no load wheel angular velocity (radians/second).

$V_{bm} \triangleq$ maximum motor back emf in volts.

$n \triangleq$ gear ratio.

Equation (4) shows that current is independent of any fixed gear ratio that might be chosen since torque T_{mm} varies inversely and speed ω_{mm} varies directly with the gear ratio. If the design is constrained to an armature-controlled dc motor with fixed-field excitation (e.g., PM), fixed supply voltage, and fixed winding configuration, then the maximum current is independent of the gear ratio. This result is interesting because simplicity of design and/or reliability makes these constraints desirable. Furthermore, the maximum current requirement is an essential and critical design parameter that must be known in the design of the control electronics.

Battery Voltage Selection

Using equation (4) to determine the MLRV motor current requirement, the maximum torque and speed are known; thus, only the voltage available for back emf can be varied. Since minimum current is desirable from controller design considerations, a large battery voltage is required; however, maximum battery voltage is bounded by voltage ratings of semiconductors used in the controller. Experience in the Saturn-Apollo reliability program has led to the use of 100-percent derating of electronic components as a guideline. This requirement limits the battery voltage to between 35 and 40 V for maximum use of flight qualified semiconductors. Discussions with battery designers indicate that with the silver-zinc battery, an open circuit beginning-of-life voltage of about 38 V and operating life voltage of about 34 V are good compromises for this application. When the V_c drop (Fig. 2) is considered, approximately 32 V are available for V_b . Using this, the vehicle stall torque, and the no-load speed parameters in equation (4) gives maximum current

$$I_{mm} = \frac{88 \times 11}{32} = 30 \text{ A.}$$

Motor-Power Train Tradeoff

Even though the motor current required is independent of gear ratio, the motor weight is not, and a tradeoff between motor weight and power train weight is needed. Motor weight is in general a complicated function of several parameters and somewhat subjective as to the relative importance of these parameters. However, a study of existing designs shows that the two most important factors affecting weight are stall torque and power dissipation. By using a heuristic approach,⁴ an empirical formula was developed relating weight to those two factors.

$$W_m = \frac{K_m T_{mm}}{\sqrt{P_{mm}}} \quad (5)$$

where

T_{mm} - maximum stall torque in newton meters.

P_{mm} - maximum I^2R power dissipated in motor (watts).

W_m - weight of motor in kg.

K_m - a constant $\sqrt{\frac{\text{watts}}{\text{meter}}}^5$.

This formula is not to be understood as a motor design equation, but as a system design tool for tradeoff studies. The torque, T_{mm} , of the motor is a function of the gear ratio, n , and T_{wm} ; i.e.,

4. Also from private discussions with G. Auclair, General Electric Co.

5. For the type motor assumed, K_m has been determined from empirical data

to be approximately $5.15 \sqrt{\frac{\text{watts}}{\text{meter}}} \quad \left(15.4 \sqrt{\frac{\text{watts}}{\text{ft}}} \right)$.

$$T_{mm} = \frac{T_{wm}}{n} . \quad (6)$$

Making this substitution into equation (6) gives

$$W_m = \frac{5.15 T_{wm}}{n \sqrt{P_{mm}}} . \quad (7)$$

Substituting the MLRV parameters into equation (7) gives

$$W_m = \frac{454}{n \sqrt{P_{mm}}} . \quad (8)$$

For a better understanding of the motor-gear tradeoff, a family of curves is drawn using equation (8) and is shown in Figure 3. Motor weight is shown as a function of gear ratio with maximum power dissipated per kilogram of motor as a parameter. These curves show that an increase in gear ratio above 10:1 does not significantly reduce motor weight. The weight of gears increases rapidly with larger ratios so that the best motor weight tradeoff appears to occur at a gear ratio of about 10:1. There are additional reasons to select a low gear ratio. Gear wear increases with ratio because of the increased linear travel of the gear. Studies at MSFC [5] on gear lubrication indicate that ratios higher than 10:1 would make dry lubricants questionable and introduce the need for wet lubricants with their attendant problems at the temperature and pressure extremes expected on the lunar surface.

MOTOR-BATTERY TRADEOFF

Determination of the optimum motor weight requires additional considerations based on the curves shown in Figure 4. A torque-speed curve for a motor (A) that will just satisfy the MLRV maximum speed and stall torque requirements is shown [resistance (A) = 1 Ω]. The power output for this motor is also plotted. A torque-speed curve for a motor (B) with a winding resistance of 0.25 Ω is also shown along with a plot of its output power. Copper losses (I^2R) for each motor are represented by the difference between the input and output power curves for the respective motor at any specific output torque.

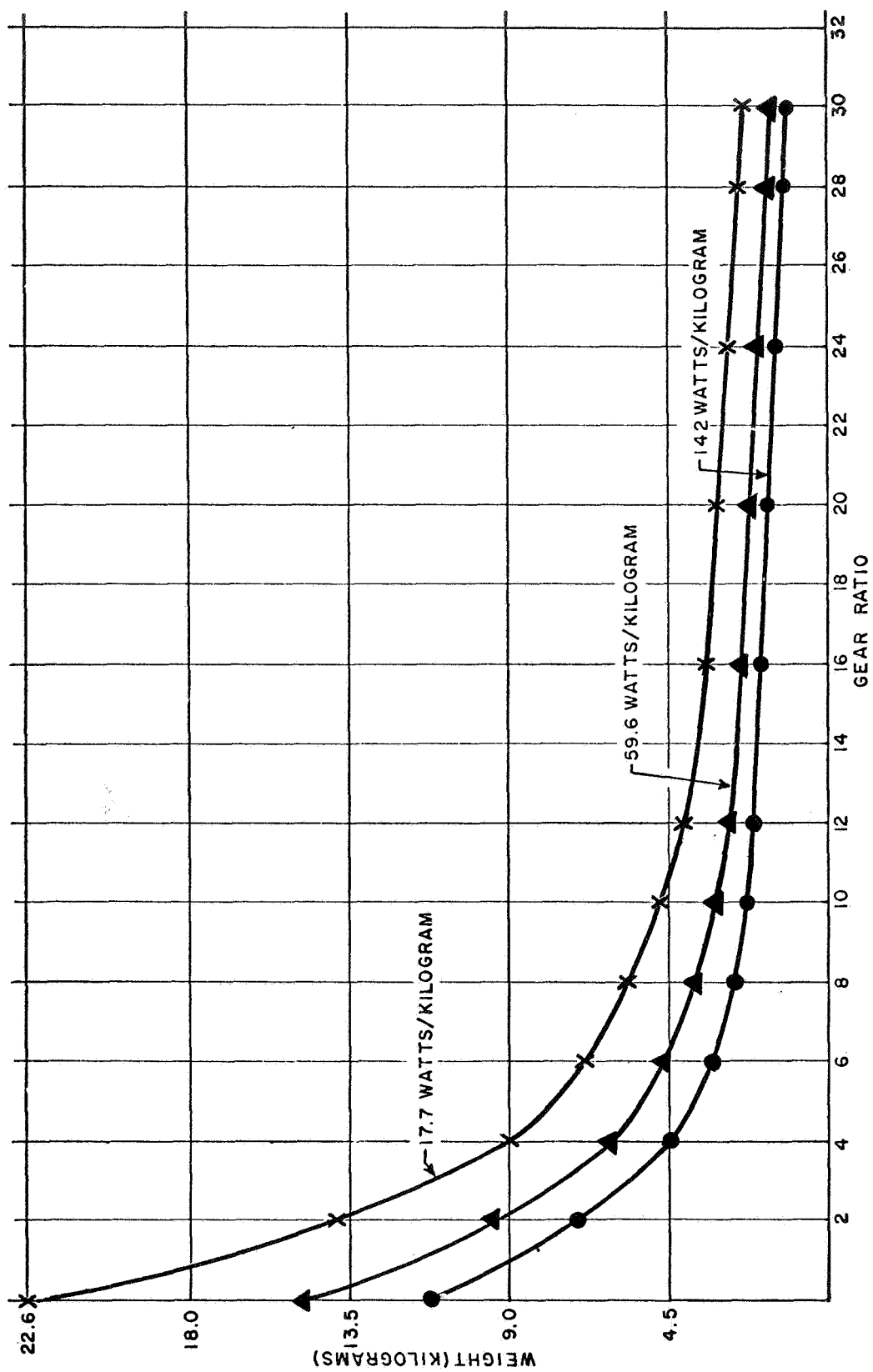


Figure 3. Motor weight versus gear ratio for MLRV.

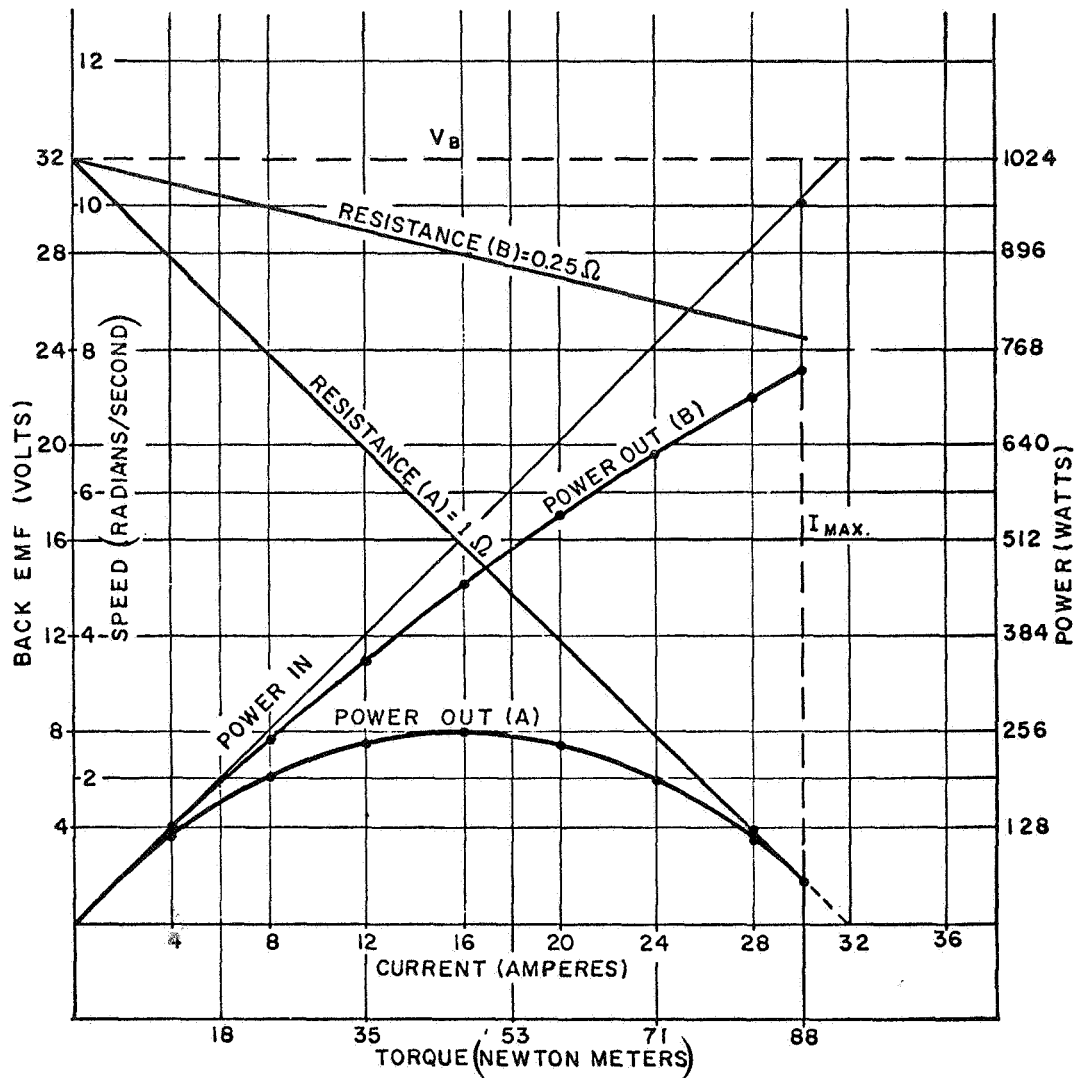


Figure 4. Torque-speed curves for dc motor.

Lower resistance would be desirable from energy considerations but would increase the weight of the motor. Notice that the 0.25Ω motor is capable of delivering maximum torque at 80 percent of maximum speed.

A tradeoff between battery and motor weight could be done more precisely with a knowledge of the power profile to be expected on the lunar surface. However, since a power profile is not available, an estimate will be made and calculations shown to demonstrate the method. Assume that during a 3-hr sortie,

an average (torque) current is one-fourth maximum for a 2-hr period. (This leaves 1 hr during which the vehicle is at rest, say for scientific tests.) In the smallest possible motor that will meet specifications (curve A of Fig. 4), the armature resistance is 1 Ω and the power dissipated for one-fourth current would be

$$P = I^2 R = \left(\frac{30}{4} \right)^2 \times 1 = 56 \text{ watts} \quad . \quad (9)$$

The energy required to supply these losses for 2 hr is 112 watt-hr. Using silver-zinc batteries with an energy density of 88 watt-hr/kg (40 watt-hr/lb), the battery weight required to supply these losses is

$$W_b = \frac{112}{80} = 1.27 \text{ kg (2.8 lb)} \quad . \quad (10)$$

Using the motor weight formula in equation (8) with n equal to 10, the motor weight is

$$W_m = \frac{454}{10 \sqrt{900}} = 1.51 \text{ kg (3.3 lb)} \quad (11)$$

This requires a motor with maximum power dissipation capability of 596 watts/kg (270 watts/lb). Experience, survey of catalog items, and discussions with motor designers indicate that a power density well below 200 watts/kg (91 watts/lb) is necessary for high reliability;⁶ therefore, a more efficient motor should be considered. By reducing the armature resistance by a factor of 4 (curve B, Fig. 4), the power (14 watts), energy (28 watt-hr), and battery weight, 0.32 kg (0.7 lb) are all reduced by this factor. The motor weight on the other hand will increase by a factor of 2; i.e., 3.03 kg (6.67 lb). Thus, overall weight has increased by 0.544 kg (1.2 lb), but maximum power dissipation is reduced to 75 watts/kg (34 watts/lb). It will be shown later that this tradeoff may also be used to reduce controller weight.

6. Assuming no cooling and operating in a vacuum.

Environmental Considerations

Thus far, the design considerations have made the tacit assumption that environmental problems can be solved; however, the effect of temperature on the design should be explored. The maximum power dissipation per kilogram is a measure of the temperature rise that can be expected in the motor during operation. Although a power profile of the mission is again necessary to obtain specific values, it is possible to bracket the design until more specific data are available.

The lunar environment is a hard vacuum and the temperature varies between $\pm 120^\circ\text{C}$. The MLRV is expected to operate only during lunar morning when the sun is between 10 and 30 degrees above the horizon; therefore the extremely low temperatures are not expected. For purposes of this study, the vehicle will be assumed to reach a temperature of 100°C . A check with motor manufacturers reveals that insulations, which are the limiting items, can be manufactured to withstand temperatures to near 250°C . Although this gives an allowable temperature excursion of 150°C , a temperature rise of more than 100°C is objectionable since it impacts the motor design in at least two different ways. First is the increase in resistance of copper with temperature that causes increased I^2R loss. For example, using the familiar formula for resistance change with temperature

$$R_2 = R_1 [1 + \alpha_1 (T - T_1)] \quad (12)$$

where

R_2 = resistance at temperature T

R_1 = resistance at temperature T_1

α_1 = temperature coefficient of resistance at T_1

$\alpha_1 = 0.00385$ at 25°C

the resistance of the motor at 200°C , assuming R_1 is 1.0Ω at 25°C , is

$$R_2 = 1 [1 + 0.00385 (200 - 25)] = 1.674\Omega .$$

This causes power dissipation to increase proportionally and could cause the motor to overheat and fail. This temperature effect should be compensated in the design by a change in motor weight if comparable operation is to be assumed. For example, the 3.03-kg (6.67-lb) motor with a resistance of 0.25Ω at 25°C would need to be reduced to 0.15Ω at 25°C to maintain the desired rating at high temperature. The motor-weight formula, equation (8), applied to the 0.15Ω design would raise the motor weight to 3.9 kg (8.6 lb).

The second impact concerns the physical design of the motor and the ability to rid itself of heat. As mentioned previously, the brushless motor has superior thermal characteristics because the winding location has a better thermal path to the vehicle. The brush-type motor must conduct the heat through its shaft and bearings and/or radiate to the stator. Since radiation is very ineffective without a large temperature differential, the brushless motor-weight penalty caused by temperature will be less than for the brush-type motor.

ADDITIONAL TECHNIQUES AND TRADEOFFS FOR REDUCING MOTOR WEIGHT AND CONTROLLER CURRENT

Previous design considerations require a maximum motor weight of about 4 kg (9 lb). Weight of the power train, battery, and controller for each wheel will add significantly to the motor weight. Since weight is a prime consideration in this design, additional possibilities for reducing the weight of the drive system are discussed.

Initial assumptions in the design did not consider a gear shift. Addition of a gear shift can reduce the operational requirements of the motor and thus reduce weight. For example, consider a simple gear shift which changes the ratio from 10:1 to 5:1 as shown in Figure 5(B). When operating along curve A, maximum torque is available, but only one-half maximum speed is attainable. Operating along curve B allows full speed but only one-half the desired maximum torque. In the 10:1 configuration the maximum rate is 5.5 rad/s which, using equation (4), yields a maximum current of

$$I_m = \frac{T_{mm} W_{mm}}{V_b} = \frac{88 \times 5.5}{32} = 15 \text{ A} \quad . \quad (13)$$

This would reduce the power dissipated per kilogram with the minimum weight motor (now 2Ω) to approximately 135 watts versus 270 watts for the previous design while also reducing the controller requirements. The disadvantage of a gear shift is the complexity, if automatic (which would be most desirable from the operational standpoint), or the increased astronaut workload for a manual shift. A gear shift would also add weight and could offset advantages gained in decreasing the motor weight.

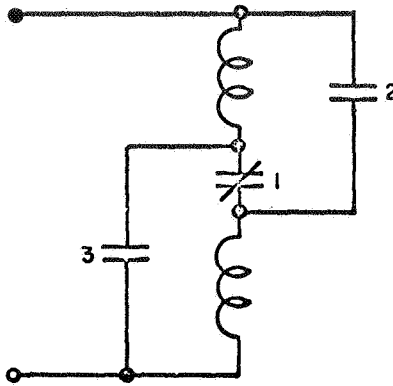
An attractive alternative is a winding shift in which two coils are wound bifilar on the motor and are capable of either series or parallel operation. A winding shift is not practical in the PM brush-type motor because of the commutation technique. Figure 5(A) shows one possible technique for changing from series to parallel operation. Figure 5(B) shows the torque-speed curves for both series and parallel winding configuration. When the windings are in series the operation is along the lines a b c d, and for parallel connection operation is along lines g c e f. Again the operation allows a reduction in controller current by one-half, but it should be emphasized that it does not reduce the power dissipation requirements for the motor.⁷ However, it does allow a smaller controller and the weight penalty of the switching is much less than would be required for a mechanical gear shift.

CONSIDERATIONS FOR THE MOTOR CONTROLLER

The motor controller is required to control efficiently torque and speed and to provide regenerative or dynamic braking for the vehicle. The amplifiers are designed with solid-state circuitry using silicon transistors and diodes as active components in both the power and low-level circuitry. Standard micro-circuits are used wherever possible.

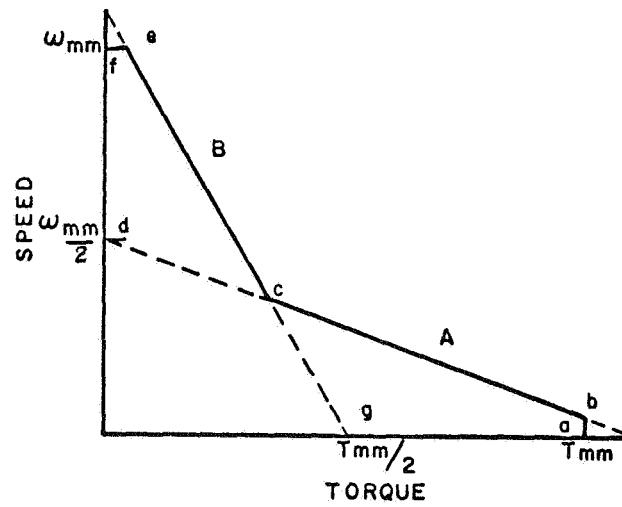
The high efficiency requirement is met by using a switching-type amplifier and pulse width modulation. With this technique, a pulse train with a period much smaller than the electrical time constant of the winding is applied

7. The power is not decreased because the number of turns must be doubled for proper torque constant. Since this would represent a double in the volume of copper, the wire size must be halved to fit into the same stator. The resistance therefore goes up by 4 as the current is reduced to one-half and I^2R remains constant.



CONTACTS	1	2	3	OPERATION
	CLOSED	OPEN	OPEN	SERIES
	OPEN	CLOSED	CLOSED	PARALLEL

(A)



(B)

Figure 5. Series/parallel winding configuration.

to the motor. The pulse amplitude is constant and approximately equal to the battery voltage. The pulse width is increased or decreased as more or less torque (or speed) is commanded. A path is provided in the controller so that energy stored in the winding inductance will force the current supplied during the pulse-on period to continue flowing during the pulse-off period, resulting in continuous smooth motor current. With this type of amplifier, all power transistors are either switched fully off (dissipating no power) or fully on (dissipating little power), resulting in high efficiency operation.

Figure 6(A) is a simplified schematic of the electronics for driving one phase of a Hall effect motor. A speed input command will cause an excitation current to flow in the Hall device, resulting in a Hall output voltage. This voltage is amplified and summed with a triangular wave in a transformer, which is a part of the pulse width modulator. As shown in Figure 6(B), both outputs of the modulator are zero for zero input signal. Positive input causes a pulse train at V_{01} and a negative input causes a pulse train at V_{02} .

The power bridge is biased such that transistors Q_3 and Q_4 are full-on and Q_1 and Q_2 are full-off for zero input (zero output from the modulator). An input pulse from V_{01} will invert Q_1 and Q_3 (Q_2 and Q_4 remain unchanged), allowing current to flow from the battery through Q_1 , the motor, and Q_4 . When the pulse returns to zero, Q_1 switches off and energy stored in the winding inductance forces the current to continue flowing or to "free-wheel" through the path provided by Q_4 , R_2 , and diode D_1 . As indicated in the curve of Figure 6(C), for small duty cycles, the average current supplied by the battery is much less than the continuous current flowing in the motor. Motor current (and hence torque) are reversed by an input pulse train from V_{02} .

The voltage developed across resistors R_1 or R_2 (normally milliohm resistors) is directly proportional to the motor current. This voltage is fed back and summed with the Hall output voltage. Motor current is commanded by the magnitude of the Hall voltage and is forced by the feedback loop to the commanded value regardless of changes, within specified limits, in battery voltage, motor resistance, or motor back emf. Since the Hall output voltage is limited to a given value, full-stall torque can be continuously developed in a motor and the current will be limited to a safe value determined by the maximum Hall voltage. Efficient operation, with this type of amplifier driving the motor of Figure 4, curve B, now becomes apparent. At full-stall torque, the motor is producing no useful work; hence the battery should supply only the I^2R losses of the motor. If 30 A are commanded ($R_m = 0.25 \Omega$), these losses are 225 watts. Since this is being supplied from a 30-V source, the average

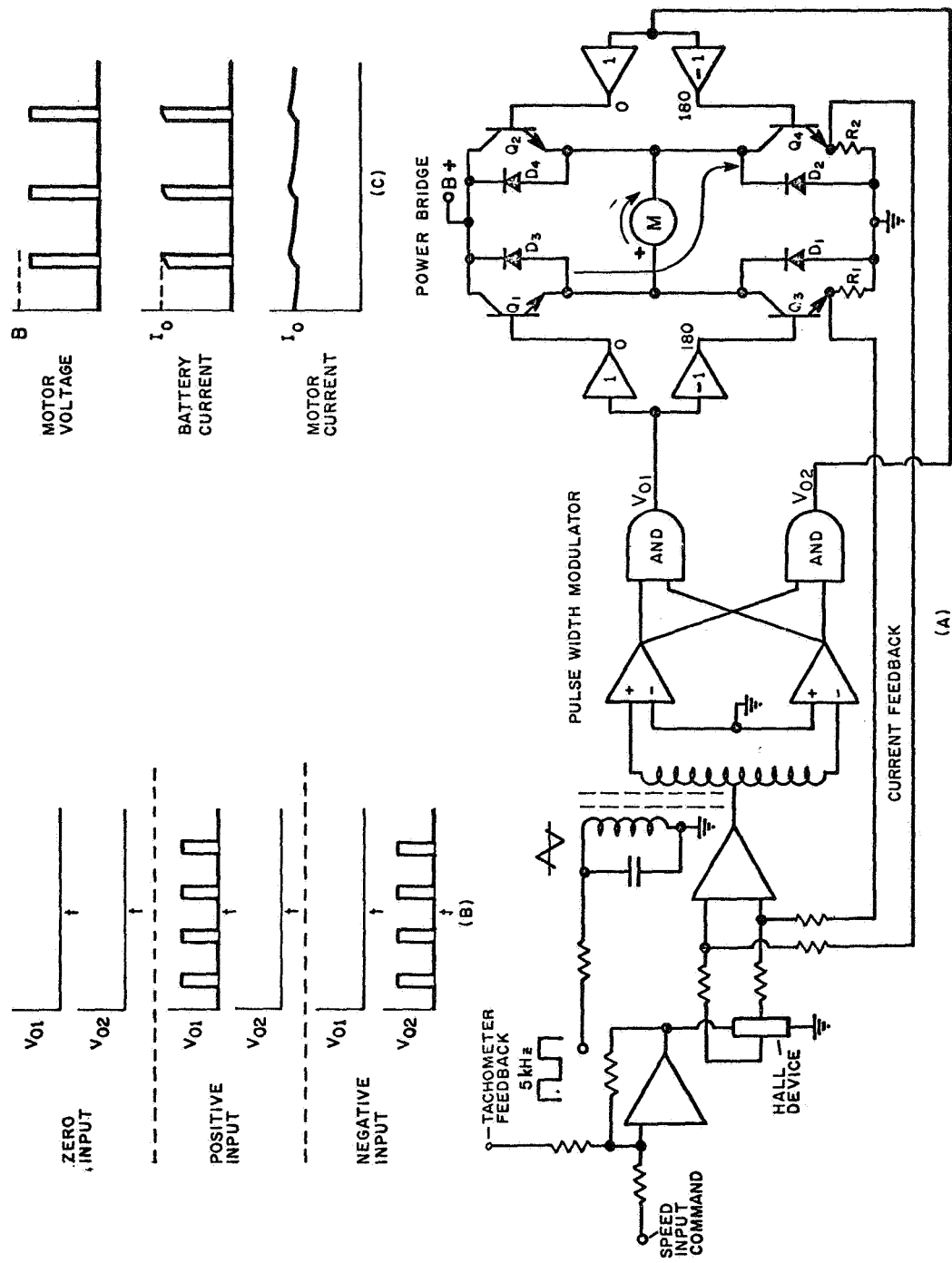


Figure 6. Motor controller.

current taken from the battery will be $225/30$ or 7.5 A. The current feedback loop will adjust the width of the voltage pulses from the modulator to a 25-percent duty cycle to maintain 30 A in the motor. As the motor speed and back emf increase, the drop in current is detected by resistors R_1 and R_2 . The error signal increases at the summing input, increasing the pulse width, and maintains motor current at the commanded value. The increase in average battery current multiplied by the battery voltage represents the useful output of the motor.

If the 1Ω motor shown in Figure 4 is used, the I^2R losses of the fully stalled motor developing maximum torque are 900 watts. To supply this loss, the output of the amplifier would adjust to a 100-percent duty cycle and the average battery current and motor current would be equal. Since the amplifier voltage is limited by the battery, 30 A cannot be maintained as back emf is developed, and the torque decreases as the speed increases.

The current feedback loop that provides the control for acceleration also controls deceleration and regenerative braking. Assume the direction of rotation and back emf are as indicated in Figure 6(A). The back emf opposes the battery voltage when the motor is accelerated. For deceleration or dynamic braking, current must be driven through the motor in a direction opposite to that indicated by the arrow. A reversal command will cause a pulse train out of V_{02} , which turns Q_2 on and Q_4 off. Back emf now aids the battery voltage and the current rises rapidly through Q_2 , the motor, Q_3 , and R_1 . Transistor Q_2 is turned off when the input command is nulled out by the voltage developed across R_1 . However, the normal position of Q_3 is on and the back emf causes the motor current to continue to build up through Q_3 , R_1 , and D_2 . This is instantaneously sensed by R_1 , reversing the summing amplifier output and creating a pulse out of V_{01} that turns off Q_3 . The energy stored now forces the current back through the battery by the path provided by diodes D_3 and D_2 .

Dynamic braking is a requirement of the LRV. Experience has shown that this system when driving an efficient motor (95 percent at rated speed) can return approximately 33 percent of the energy stored in an inertia load back to a 28-V battery. This energy conservation may or may not be an important consideration in the LRV application. It is not certain at this time whether the high energy density batteries that will be used can accept the number of recharge cycles that will be encountered in the operation of the vehicle. In the event current cannot be returned to the source, additional circuitry will be required to detect the current reversal and large power resistors will be switched in to dissipate the energy.

It was stated earlier that it is desirable to reduce the current in the controller. In addition to increasing reliability, this will significantly reduce the volume and weight of the controller. As indicated in Figure 6(A), eight power transistors and eight power diodes are required per motor. (A controller is required for each phase.) Transistors capable of controlling 30 A with a sufficient current gain at the extreme cold temperature of the lunar environment would nominally be rated at 100 A. The cases of transistors this size normally occupy between 15 and 30 cm³. When mounted to a heat sink, a large heavy package results. The lower current attainable by switching windings in the motor permits the use of smaller devices and will significantly reduce the weight and volume of the controller.

APPENDIX A

THE BRUSHLESS DC MOTOR

Many techniques have been developed for designing brushless dc motors, including both two-phase and three-phase machines. In these motors, the commutator and brushes are replaced by a rotor position sensor, and the rotor is generally a PM. Angular position information from the rotor sensor is used to drive current into the stator windings with the proper phase to generate a torque that is independent of rotor position.

Three-phase motors generally use an off-on type of sensor, such as a photodiode switch or a variable reluctance switch, which results in a square wave of current being applied to the windings. The three-phase operation minimizes losses caused by the third harmonic content in the square wave.

In the two-phase machine, the rotor position is resolved into a sine and cosine function through the use of either Hall effect devices or brushless resolvers. The position signal is linearly amplified to produce sinusoidal currents in the stator windings. With this type of motor, ripple torques on the order of 5 percent are practical whereas a 10-percent ripple torque can be expected with the square-wave techniques used in the three-phase machines. Ripple torque is not an important consideration for the LRV; however, the two-phase motor is preferred because of the simpler control system required. In the following paragraphs, the operation of a two-phase Hall effect brushless motor is discussed.

A Hall effect device is a small slab of silicon on which a thin film of indium arsenide or indium antimonide has been deposited with input and output leads attached as shown in Figure A-1. If a current is passed between the two input leads and a magnetic field cuts through the device perpendicularly to the current flow, the flux deflects the charge carriers, producing a voltage at the two output leads. The magnitude of this Hall voltage is given by $V_h = K_h IB$ where K_h is the Hall constant, I is the current applied, and B is the flux produced by the PM rotor.

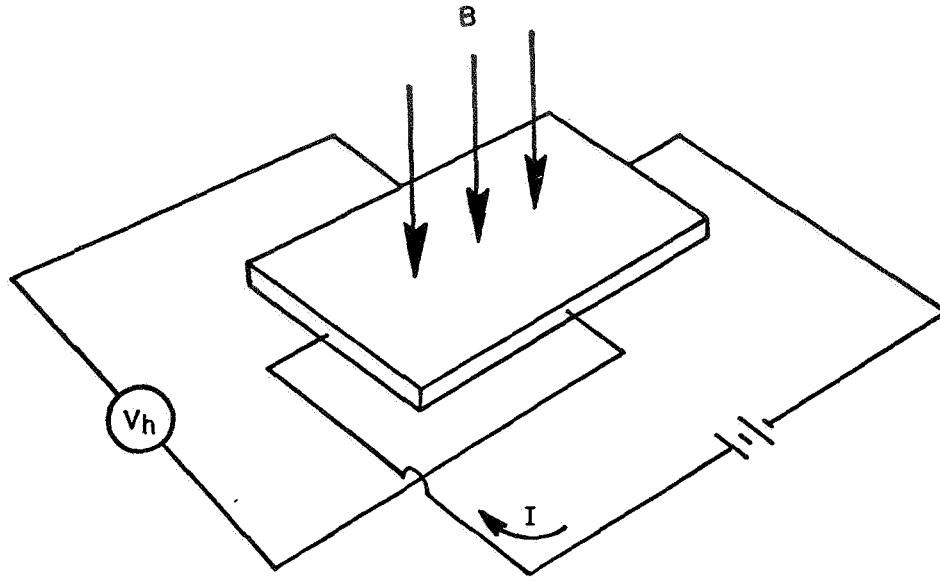


Figure A-1. Hall effect device.

Figure A-2 illustrates the principle of motor operation. The motor shown has a two-pole PM rotor and a two-phase winding with each phase displaced 90 electrical degrees. A sensing rotor is mounted on the motor shaft with its poles aligned with the poles of the main rotor. Two Hall devices, displaced 90 degrees and aligned to the pole center of each phase, are mounted in the airgap of the sensing rotor.

If a constant excitation current is applied to the Hall devices and the shaft is turned, the output voltages are

$$V_{h_1} = K_h I_{ex} B \sin \alpha = V_h \sin \alpha \quad (A-1)$$

$$V_{h_2} = K_h I_{ex} B \cos \alpha = V_h \cos \alpha \quad (A-2)$$

and the torque produced by each winding is

$$T_1 = K_t I_1 \sin \alpha \quad (A-3)$$

$$T_2 = K_t I_2 \cos \alpha \quad (A-4)$$

where K_t is a machine constant.

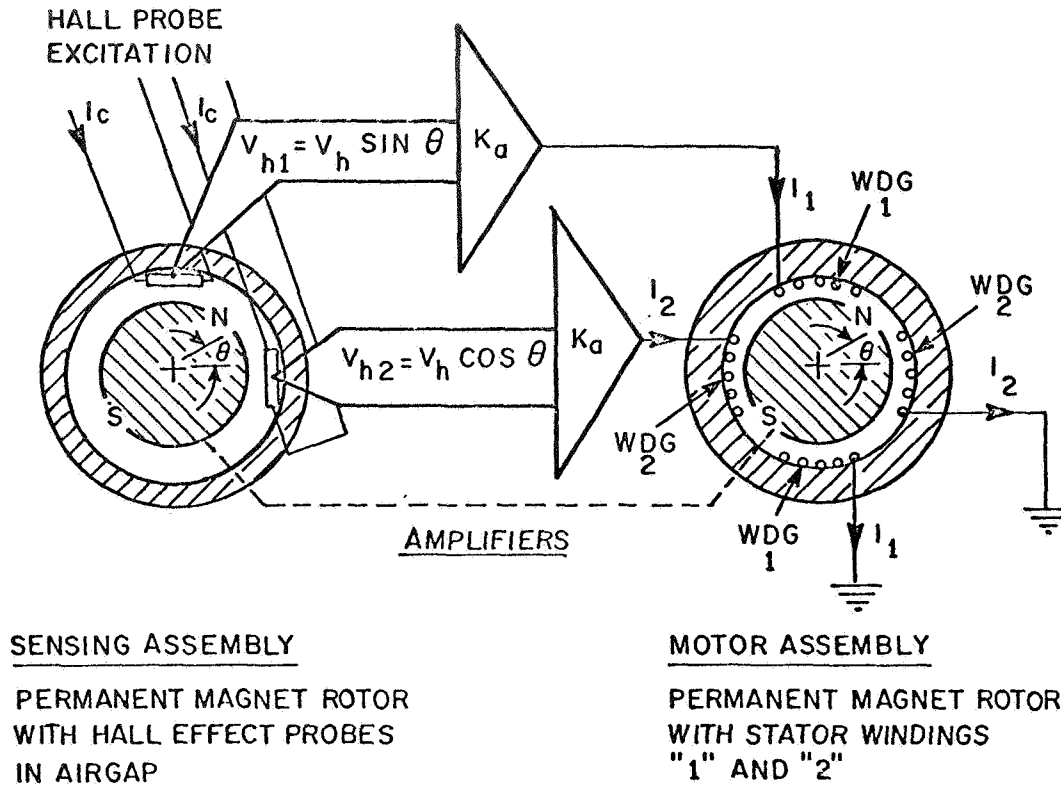


Figure A-2. Basic operation of motor.

Since the winding currents, I_1 and I_2 , are functions of the amplified Hall voltages, equations (A-1) and A-2) may be substituted into equations (A-3) and (A-4) respectively to give

$$T_1 = K_t (V_h \sin \alpha K_a) \sin \alpha = K_t K_a V_h \sin^2 \alpha \quad (\text{A-5})$$

$$T_2 = K_t (V_h \cos \alpha K_a) \cos \alpha = K_t K_a V_h \cos^2 \alpha \quad (\text{A-6})$$

where K_a is the amplifier gain in amperes/volt.

The total torque is the sum of the torque produced by each phase.

$$T = T_1 + T_2 = K_t K_a V_h (\sin^2 \alpha + \cos^2 \alpha) = K_t K_a V_h \quad (\text{A-7})$$

which is independent of rotor position. Thus, both the magnitude and direction of the torque may be controlled by varying the magnitude and direction of the excitation current for the Hall devices.

If the extreme temperature of the lunar surface precludes the use of Hall devices for position sensing, then a resolver mounted and properly aligned on the motor shaft will produce the required sine and cosine functions. The motor operation is identical to that described previously with the exception that additional modulation and demodulation circuitry is required to properly condition the resolver excitation and output voltage.

The rotor position signals present in brushless motors may be used to obtain odometer information. By detecting and counting the sinusoidal cross-overs, the motor revolutions (and hence distance traveled) can be determined. Information contained in the sine and cosine functions may also be used to determine the direction of rotation.

Another interesting aspect of the brushless motor is the possibility for constructing a brushless dc tachometer. If the rotor is driven by an external source, sinusoidal voltages proportional to speed are developed across each phase of the motor windings (Fig. A-2). These phase voltages are given by

$$V_{s1} = K_w \dot{\alpha} \sin \alpha \quad (A-8)$$

$$V_{s2} = K_w \dot{\alpha} \cos \alpha \quad (A-9)$$

where K_w is a machine constant with dimensions of volts/radians/second. It has been shown that, for fixed excitation current, the Hall output voltages are

$$V_{h1} = K_h I_x B \sin \alpha \quad (A-10)$$

$$V_{h2} = K_h I_x B \cos \alpha \quad (A-11)$$

If the output from winding No. 1, equation (A-2), is connected to the input of Hall device No. 1, equation (A-2), then the Hall device output is given by

$$V_{h1} = \left(\frac{K_w \dot{\alpha} \sin \alpha}{R_1} \right) K_h B \sin \alpha \quad (A-12)$$

$$V_{h2} = \left(\frac{K_w \dot{\alpha} \cos \alpha}{R_2} \right) K_h B \cos \alpha \quad (A-13)$$

where R_1 and R_2 are the respective stator winding resistances.

The sum of two Hall device outputs (V_o) is, assuming $R_1 = R_2$,

$$V_o = \frac{K_w K_h \dot{\alpha} B}{R} (\sin^2 \alpha + \cos^2 \alpha) \quad (A-14)$$

$$V_o = K_b \dot{\alpha} \quad (A-15)$$

and K_b is the tachometer gradient with dimensions of volts/radians/seconds. The same technique may be used with the brushless resolver, the significant difference in mechanization being the additional signal conditioning circuitry required for the resolver.

REFERENCES

1. Parker, Rollin J.; and Studders, Robert J.: Permanent Magnets and Their Application. General Electric Co., John Wiley & Sons, Inc., p. 21.
2. Slabiak, Walter; and Collins, George C.: Brushless Synchronous Motor. Soc. Automotive Engrs., 680455, May 20-24, 1968.
3. Manteuffel, E. W.: Direct Current Brushless Torquer. Final Report, Contract NAS8-11658, MSFC, Huntsville, Alabama, May 1965.
4. Auclair, G. F.; Manteuffel, E. W.; and Rosenlieb, J. W.: Brushless DC Spin Motor for Momentum Exchange Attitude Control, Final Report, Contract NAS8-20591, MSFC, Huntsville, Alabama, December 1967.
5. Demorest, K. E.: An Investigation of Dry Lubricated Gears for Use in Vacuum. Paper presented at Conference on Solid Lubricants, Sponsored by Air Force Materials Laboratory and Midwest Research Institute (Kansas City, Missouri) Sept. 9-11, 1969, to be published in Proceedings of AFML-MRT Conference on Solid Lubricants 1970.

APPROVAL

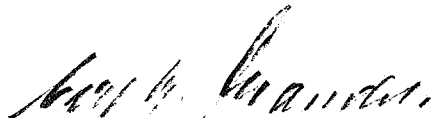
TM X-53972

TRACTION DRIVE SYSTEM DESIGN CONSIDERATIONS FOR A LUNAR ROVING VEHICLE


By Clyde S. Jones, Jr., Billy J. Doran, and Frank J. Nola

The information in this report has been reviewed for security classification. Review of any information concerning Department of Defense or Atomic Energy Commission programs has been made by the MSFC Security Classification Officer. This report, in its entirety, has been determined to be unclassified.

This document has also been reviewed and approved for technical accuracy.



CARL H. MANDEL
Chief, Guidance and Control Division



F. B. MOORE
Director, Astrionics Laboratory

DISTRIBUTION

TM X-53972

INTERNAL

DIR

DEP-T

PM-SAT

Mr. Morea

PD-AP

Mr. Stewart

Mr. Wales

Mr. Currie

S& E-ASTN-M

Mr. Demorest

S& E-CSE-DIR

Dr. Haeussermann

S& E-ASTR-DIR

Mr. Moore

Mr. Horton

S& E-ASTR-A

Mr. Hosenthien

Miss Flowers

S& E-ASTR-C

Mr. Swearingen

S& E-ASTR-E

Mr. Aden

INTERNAL (Continued)

S& E-ASTR-G

Mr. Mandel

Dr. Doane

Mr. Kalange

Mr. Kelley

Mr. Broussard

Mr. Jones (25)

Mr. Doran

Mr. Nola

Mr. Berry

Mr. White

Mr. Burch

Mr. Wales

Mr. LeBas (Sperry)

Mr. Wajnberg (Sperry)

S& E-ASTR-I

Mr. Powell

S& E-ASTR-M

Mr. Boehm

S& E-ASTR-R

Mr. Taylor

S& E-ASTR-S

Mr. Wojtalik

Mr. Brandner

S& E-ASTR-ZX

Central File

AD-S

PM-PR-M

DISTRIBUTION (Concluded)

INTERNAL (Concluded)

A&TS-MS-H

A&TS-MS-IP (2)

A&TS-MS-IL (8)

A&TS-TU (6)

A&TS-PAT

Mr. L. D. Wofford, Jr.

EXTERNAL

Scientific and Technical Information Facility (2)

P. O. Box 33

College Park, Maryland 20740

Attn: NASA Representative (S-AK/RKT)

Dr. E. Manteuffel

Defense Electronics Division

Avionic Controls Department

General Electric Company

Binghamton, New York 13900